How Gastric Lipase, an Interfacial Enzyme with a Ser-His-Asp Catalytic Triad, Acts Optimally at Acidic pH

Henri Chahinian,[‡] Torben Snabe,[§] Coralie Attias,[‡] Peter Fojan,[§] Steffen B. Petersen,[§] and Frédéric Carrière*[,‡]

Laboratoire d'Enzymologie Interfaciale et de Physiologie de la Lipolyse, CNRS UPR 9025, IBSM, Marseille, France, and Biostructure and Protein Engineering, Institute of Physics and Nanotechnology, Aalborg University, Denmark

Received September 15, 2005; Revised Manuscript Received November 5, 2005

ABSTRACT: Gastric lipase is active under acidic conditions and shows optimum activity on insoluble triglycerides at pH 4. The present results show that gastric lipase also acts in solution on vinyl butyrate, with an optimum activity above pH 7, which suggests that gastric lipase is able to hydrolyze ester bonds via the classical mechanism of serine hydrolases. These results support previous structural studies in which the catalytic triad of gastric lipase was reported to show no specific features. The optimum activity of gastric lipase shifted toward lower pH values, however, when the vinyl butyrate concentration was greater than the solubility limit. Experiments performed with long-chain triglycerides showed that gastric lipase binds optimally to the oil−water interface at low pH values. To study the effects of the pH on the adsorption step independently from substrate hydrolysis, gastric lipase adsorption on solid hydrophobic surfaces was monitored by total internal reflection fluorescence (TIRF), as well as using a quartz crystal microbalance. Both techniques showed a pH-dependent reversible gastric lipase adsorption process, which was optimum at pH 5 (K_d = 6.5 nM). Lipase adsorption and desorption constants (k_a = 147 860 M^{-1} s^{-1} and $k_d = 139 \times 10^{-4}$ s^{-1} at pH 6) were estimated from TIRF experiments. These results indicate that the optimum activity of gastric lipase at acidic pH is only "apparent" and results from the fact that lipase adsorption at lipid−water interfaces is the pH-dependent limiting step in the overall process of insoluble substrate hydrolysis. This specific kinetic feature of interfacial enzymology should be taken into account when studying any soluble enzyme acting on an insoluble substrate.

Gastric lipase is active and stable in the acidic environment of the stomach, where the gastrointestinal (GI)[1] lipolysis of dietary fat is initiated (*1*). This lipase can be said to be an extremophilic enzyme because it retains its activity in gastric juice at pH 2 and physiological temperature (*2*). Dog gastric lipase is the lipase showing the highest hydrolytic activity on long-chain triglycerides at low pH levels, with an optimum activity at pH 4 (*3*). In addition, gastric lipase is not inhibited by the bile salts present in the GI tract, whereas pancreatic lipase, the main lipase involved in fat digestion, requires a cofactor, namely colipase, to counteract the inhibitory effects of bile salts on lipase adsorption at lipid−water interfaces (*4*).

Like that of other lipases, the 3D structure of gastric lipase is based on an α/β hydrolase fold and its active site, which is covered by an amphiphilic lid domain, comprises a Ser-His-Asp catalytic triad and an oxyanion hole (*5*, *6*). Most lipases show optimum activity at pH levels above 7, which is consistent with the ionization properties of histine (pK_a = 6.5) and the fact that this residue is known to play an important role in the charge relay system involving the catalytic triad and the enhancement of the nucleophilic character of the serine residue. It was therefore of great importance to understand the unusual optimum activity of gastric lipase occurring at acidic pH values, and many efforts have been made to perform structural studies for this purpose. The 3D structures of human (HGL) and dog (DGL) gastric lipases were not found, however, to show any specific features at the level of the catalytic triad, which was superimposable on all of the catalytic triads observed in other lipases and esterases thus far (*5*, *6*). One might expect the catalytic histidine residue His353 to show a strong local pK_a decrease to explain the acidic pH optimum of gastric lipase. No additional charged residues were observed within a 10-Å sphere centered on the active-site Ser153 Oγ atom, and long-distance interactions with residues present outside this sphere could not be established. It was therefore impossible to postulate any mechanism for a local change in the histidine pK_a.

Lipases are soluble enzymes that act on a natural insoluble triglyceride substrate and therefore perform interfacial catalysis. This catalytic process can be described in terms of a lipase adsorption step occurring at the oil−water interface, followed by the formation of an interfacial enzyme−substrate complex and the release of lipolysis products (*7*). Contrary to what is observed with "classical" enzymes acting on

* To whom correspondence should be addressed: Laboratoire d'Enzymologie Interfaciale et de Physiologie de la Lipolyse, CNRS UPR 9025, 31 chemin Joseph Aiguier, 13402 Marseille cedex 20, France. Telephone: (33) 4 91 16 41 34. Fax: (33) 4 91 71 58 57. E-mail: carriere@ibsm.cnrs-mrs.fr.

‡ CNRS UPR 9025.

§ Aalborg University.

[1] Abbreviations: GI, gastrointestinal; HGL, human gastric lipase; NaTDC, sodium taurodeoxycholate; QCM, quartz crystal microbalance; rDGL, recombinant dog gastric lipase; S, concentration corresponding to the substrate solubility limit; TIRF, total internal reflection fluorescence; VC4, vinyl butyrate.

10.1021/bi0518803 CCC: $33.50
Published on Web 12/24/2005

soluble substrates, the kinetic properties and substrate specificity of interfacial enzymes can result from both the adsorption of the enzyme at the lipid−water interface and the interactions occurring between the substrate and the active site. The effects of physicochemical parameters such as the pH on the enzyme turnover have mostly been studied in connection with the structural features of the active site. The pH dependency of lipase adsorption has been mainly investigated from the point of view of enzyme immobilization for biotechnological processes, but little attention has been paid thus far to the catalytic mechanism (*8*).

In the present study, we first investigated the effects of the pH level on the hydrolytic activity of recombinant dog gastric lipase (rDGL) on a partly soluble substrate (vinyl butyrate, VC4) and a completely insoluble substrate (long-chain triglyceride emulsion). The pH-dependent partitioning of rDGL between the water phase and the oil−water interface was then investigated using liquid−liquid phase separation procedures. To study lipase adsorption independently of the process of substrate hydrolysis, the pH-dependent adsorption of rDGL on solid hydrophobic surfaces was monitored by total internal reflection fluorescence (TIRF), as well as using a quartz crystal microbalance (QCM).

EXPERIMENTAL PROCEDURES

Production and Purification of rDGL. rDGL was produced in a transgenic maize by Meristem Therapeutics S. A. (Clermont-Ferrand, France) and purified as previously described (*6*).

Lipase Activity Measurements Using the pH-stat Technique. rDGL activity was determined by measuring the free fatty acids released from a mechanically stirred emulsion of either VC4 (puriss grade from Fluka) or Intralipid (30% Intralipid from Amersham Pharmacia). Using a pH-stat (TTT 80 Radiometer, Copenhagen, Denmark), the free fatty acids were automatically titrated with 0.1 N NaOH at a constant pH value in the 2−8 pH range. Each reaction with the VC4 substrate was performed in a thermostated vessel (37 °C) containing various amounts of VC4 and 15 mL of 2.5 mM Tris, 150 mM NaCl, and 0.1 μM BSA buffer. Reactions with the Intralipid substrate were performed in a thermostated vessel (37 °C) containing 5 mL of Intralipid and either 10 mL of 150 mM NaCl and 2 mM sodium taurodeoxycholate (NaTDC) solution for both lipase activity and partitioning measurements in the same assay or 10 mL of 150 mM NaCl, 3.5 mM $CaCl_2$, and 30 μM BSA solution for measuring maximum activities under optimized assay conditions (*3*). When the VC4 substrate was used, the activities directly measured with the pHstat were multiplied by a correction factor taking into account the state of ionization of the free butyric acid ($pK_a = 4.54$) at the various pH values tested. When the Intralipid substrate was used, activity measurements were performed only by back-titrating long-chain free fatty acids at pH 9, after incubating the emulsion with the enzyme for 2 min at a given pH. At each pH level used for the incubation step, a control assay was performed without any enzyme to determine the amounts of NaOH required to reach pH 9 without performing free fatty acid titration.

Binding of rDGL to Long-Chain Triglyceride Emulsions. The interfacial binding behavior of rDGL to long-chain triglycerides was investigated by mixing the enzyme with an Intralipid emulsion formed in a pHstat vial and by further measuring the lipase activity remaining in the water phase after the separation of the oil phase. The pH-stat vial thermostated at 37 °C was filled with 5 mL of 30% Intralipid (Amersham-Pharmacia, Sweden) and 10 mL of 150 mM NaCl and 2 mM NaTDC solution. The vial was placed on the automatic titrator (TTT 80 Radiometer, Copenhagen); its contents were stirred mechanically; and the pH value was adjusted at 2−7 by the addition of 0.1 N NaOH. A total of 100 μL of a 10 mg/mL rDGL solution was then added to the emulsion, and after 2 min of incubation, the contents of the pH-stat vial were transferred into a puncturable 25 × 64 mm centrifuge tube (Beckman Ultra-Clear). Satisfactory phase separation was obtained after performing centrifugation at 10 000 rpm for 60 min, at room temperature. The oil phase accumulated at the top of the tube, and a sample (2−3 mL) of the aqueous phase was recovered by introducing a 0.8 × 40 mm needle equipped with a 5-mL syringe into the bottom of the tube. The amounts of lipase remaining in the solution were determined by measuring the residual lipase activity in an aliquot of the aqueous phase using the standard rdGL assay with tributyrin as a substrate (*3*). Control assays were performed using 13 mL of buffer without any Intralipid to determine the maximum lipase activity that could be recovered from the water phase. It was checked that the lipase activity (U) introduced into each control sample was stable and could be recovered at pH values ranging from 2 to 7. Before each experiment, the pH-stat vial was washed successively with acetone, ethanol, and Milli-Q water.

TIRF Experimental Device. A TIRF system (BioElectroSpec, Inc., Harrisburg, PA) coupled with a fluorescence spectrophotometer (PTI QM-2000 from Photon Technology Int., Lawrenceville, NJ) with a 75 W Xenon arc source was used. The PTI instrument excitation and emission slits were set at 6 nm. The sample in the flow chamber was excited at 280 nm, and the fluorescence emission intensity was monitored at 330 nm. Because only proteins at the surface and those located in close proximity to the surface are excited using the TIRF setup, the resulting fluorescence emission intensity at 330 nm was used as a relative measurement of protein adsorption. The flow chamber consisted of a "sandwich" comprising a TIRF quartz prism, a TIRF quartz slide (see the method of preparation below), a 10 μm gasket (determining the flow chamber thickness), and a back block containing holes to channel the solution through the flow chamber. Further details of the TIRF theory and the specific setup used can be obtained in ref *9*.

Surface Preparation of TIRF Quartz Slides. Hydrophobic quartz slides were prepared by performing silanization as described in ref *9*. Prior to silanization, the slides were cleaned by immersing them in chromosulfuric acid at 70−75 °C for 1 h and thoroughly rinsed in water at room temperature. The slides were then hydroxylated to increase the number of OH groups present on the quartz surface. Hydroxylation was performed by immersing the slides for 1 h at 99−100 °C in 5% (w/v) potassium persulfate solution prepared in deionized water. After the slides were hydroxylated, they were flushed with deionized water and quickly dried under nitrogen. The quartz slide was then methylated by incubating the surface with 0.3% (v/v) dichlorodimethylsilane (Fluka) in trichloroethylene for 30 min at room temperature (*10*). The surface was subsequently rinsed in

pure trichloroethylene for 5 min and thoroughly flushed with ethanol and deionized water before being dried under nitrogen.

TIRF Experiments. The quartz slide and the TIRF quartz prism were pasted together using a drop of glycerol placed between them (glycerol and quartz have almost equal refractive indices and let the light pass with minimum interference). The TIRF flow chamber was prepared by placing the 10 μm gasket (polyurethane) between the quartz slide and the back block. The flow chamber was mounted vertically in the instrument, and the buffer (10 mM citrate for experiments performed at pH 4−7; 10 mM phosphate for pH 2 and 3) was run through the chamber to purge it at a flow rate of 250 μL/min. Before the adsorption experiments were performed, the surface was hydrated using the buffer containing 150 mM NaCl and 2 mM NaTDC, without any protein for 5−10 min. The rDGL solution (20 nM to 2 μM in the same buffer) was then injected. After 20−35 min of protein exposure, the system was rinsed in buffer without any protein for 10−20 min. 2% (v/v) Helmanex II (Hellma GmbH and Co KG, Germany) was then applied for 5 min, before again applying buffer to wash the flow chamber. All experiments were performed at 37 ± 0.2 °C.

Bulk Fluorescence Experiments. Experiments were performed on a PTI (Photon Technology Int., Lawrenceville, NJ) steady-state fluorescence spectrophotometer. The excitation wavelength was set at 280 nm, and the slit width on the instrument was set at 4 nm. Fluorescence spectra of the samples were recorded in the wavelength range of 295−400 nm. Data were recorded with the FELIX software supplied by Photon Technologies. Measurements were performed in quartz cuvettes using a 20 nM rDGL solution in either 150 mM NaCl, 2 mM NaTDC, and 10 mM citrate buffer (pH 4−7) or 150 mM NaCl, 2 mM NaTDC, and 10 mM phosphate (pH 2 and 3). All experiments were performed at 37 ± 0.2 °C.

QCM Experiments. Experiments were performed with a Quartz Crystal Microbalance and Dissipation device (Q-Sense D301) from Q-Sense AB (Göteborg, Sweden). A gold-coated quartz crystal with a fundamental frequency of 5 MHz was used. The gold surface of the QCM crystal was rendered hydrophobic by coating it with a monomolecular alkane (octadecyl) film with a terminal thiol group (−SH) covalently bound to the gold surface. Before the surface was prepared, a thorough cleaning process was conducted in which the crystal was first illuminated with UV light for 30 min and then immersed in a 1:1:5 (v/v/v) solution of H_2O_2/NH_3/deionized H_2O at 75 °C for 5 min, before being thoroughly rinsed with deionized water. The crystal was then immersed in a solution of 1 mM octadecylmercaptan in *n*-hexane for at least 2 h at room temperature (20−25 °C), rinsed in pure *n*-hexane, ethanol, and deionized water, and dried under nitrogen.

The quartz crystal, which had a diameter of 14 mm, was placed in a reaction chamber (volume, 80 μL; height, 0.5 mm), in which a rapid exchange of liquid was possible. Before applying the enzyme, the surface of the quartz crystal was hydrated with 150 mM NaCl, 2 mM NaTDC, and 10 mM citrate buffer for experiments performed at pH 4−7 and 150 mM NaCl, 2 mM NaTDC, and 10 mM phosphate buffer for experiments performed at pH 2 and 3, until a stable baseline value was achieved. Every buffer addition (0.5 mL) to the reaction chamber was monitored by gravity. Enzyme addition in the measurement chamber was also performed by applying 0.5 mL of a 200 nM rDGL solution into the same buffer, for 3−5 s. All experiments were performed at 32 ± 0.2 °C. After the buffer was replaced by the rDGL solution, changes in the crystal resonance frequency were recorded every second for 60 min. Data were recorded at the third overtone of the fundamental frequency (i.e., 15 MHz). On the basis of the hypothesis that the adsorbed mass of rDGL was rigid, thin, and homogeneously distributed, the frequency shift was converted into an adsorbed mass according to the Sauerbrey equation $\Delta m = -k\Delta f/n$, where Δm is the mass adsorbed, Δf is the change in frequency before and after adsorption, k is the crystal-dependent mass sensitivity constant ($k = 17.7$ ng cm^{-2} Hz^{-1}), and n is the overtone number ($n = 3$) (*11*, *12*). The mass was expressed in ng cm^{-2}, and the sensitivity of the QCM measurement was in the ng cm^{-2} range.

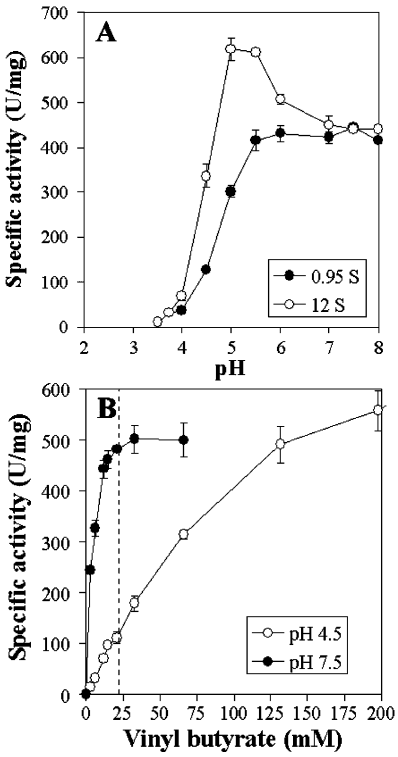

FIGURE 1: Effects of pH (A) and the substrate concentration (B) on the hydrolysis of VC4 by rDGL. (A) rDGL activity was measured as a function of the pH at two substrate concentrations corresponding to 0.95 S (soluble substrate only) and 12 S (presence of a substrate emulsion dispersed in the water phase). (B) rDGL activity was measured as a function of the substrate concentration at pH values of 4.5 and 7.5.

RESULTS

pH Profile of the rDGL Activity on VC4. The rDGL activity on the partly soluble substrate VC4 was measured as a function of the pH at two VC4 concentrations corresponding to 0.95- and 12-fold the solubility limit of VC4 (S = 22 mM). Below the substrate solubility limit (0.95 S, 20.9 mM VC4), the activity showed a sigmoidal increase with the pH and a maximum specific activity of 445 ± 7 units/mg was measured at pH 7.5 (Figure 1A). From the variation of rDGL activity on soluble VC4 with pH, it was deduced that half of the maximum activity corresponds to a pH value

of 4.8, which suggests that the pK_a of the catalytic histidine of rDGL is lower than that of histidine alone (6.5).

When VC4 was used at a concentration above its solubility limit (12 S, 264 mM), the maximum specific activity (618 ± 25 units/mg) was observed at pH 5 (Figure 1A). The activity was found to decrease at higher pH values, and at pH 7.5, it was identical to that measured with 0.95 S VC4.

Effects of the VC4 Concentration on the rDGL Activity. The rDGL activity was measured as a function of the VC4 concentration at pH 7.5 (Figure 1B), a pH value at which the activity was previously found to be poorly affected by the physicochemistry of the substrate (Figure 1A). A maximum specific activity of 500 ± 27 units/mg was measured at 33 mM VC4 (1.5 S), and the activity was measured at a VC4 concentration corresponding to 0.95-fold the solubility limit, which already reached 96% of the maximum activity (Figure 1B).

The rDGL activity was also measured as a function of the VC4 concentration at pH 4.5 (Figure 1B), a pH value at which the activity previously measured with a VC4 emulsion was found to be 2.6-fold the activity measured with soluble VC4 (Figure 1A). The specific activity of rDGL was found to increase continuously with the VC4 concentration, and the maximum activity was not reached at 200 mM VC4 (9-fold the solubility limit). The specific activity measured at a VC4 concentration corresponding to 0.95-fold the solubility limit (111 ± 11 units/mg) was only 20% of the activity measured at 200 mM VC4 (557 ± 40 units/mg; Figure 1B).

It was checked that VC4 solubility was identical at pH 4.5 and 7.5.

pH Profile of the rDGL Activity on Long-Chain Triglycerides (Intralipid). Intralipid is a fine, well-calibrated emulsion of purified soybean oil stabilized by egg yolk lecithin, which is used for parenteral nutrition. The activity of rDGL on this completely insoluble triglyceride substrate was measured as a function of the pH (Figure 2A). The maximum specific activity of rDGL under optimized assay conditions was measured at pH 4.5 and found to be half the maximum specific activity recorded with native DGL (nDGL) at pH 4 (493 ± 43 versus 966 ± 99 units/mg; Figure 2A). The activity of rDGL was also assayed with Intralipid dispersed in a 150 mM NaCl and 2 mM NaTDC solution: this solution containing bile salts was subsequently used for the measurement of rDGL adsorption onto solid hydrophobic surfaces. Under these conditions, the optimum pH for measuring the rDGL activity dropped to pH 4.0 and the maximum specific activity decreased to 232 ± 13 units/mg (Figure 2A).

rDGL Partitioning between the Water Phase and the Oil−Water Interface. After 2 min of incubation of rDGL with Intralipid dispersed in a 150 mM NaCl and 2 mM NaTDC solution at various pH levels, the water and oil phases were separated by centrifugation for at least 1 h at 10 000 rpm. The partitioning of rDGL between the water phase and the oil−water interface was assessed from the rDGL activity recovered in the water phase. The interfacial binding (%) of rDGL was deduced from these measurements and found to increase at low pH values (100% at pH 2 versus 42 ± 4% at pH 6.5; Figure 2B). The interfacial binding was not found to increase continuously, however, with decreasing pH levels in the pH range of 4−5, in which the maximum lipolytic activity was also recorded (parts A and B of Figure 3). Because partitioning could only be measured after 1 h, the results might not reflect the initial adsorption rate. The generation of lipolysis products such as long-chain free fatty acids might impair lipase adsorption with time. This possible effect might be higher at pH 4 where rDGL displays its highest activity. The partitioning of rDGL was not significantly affected when the phase separation time was extended to 2 h (Figure 2B).

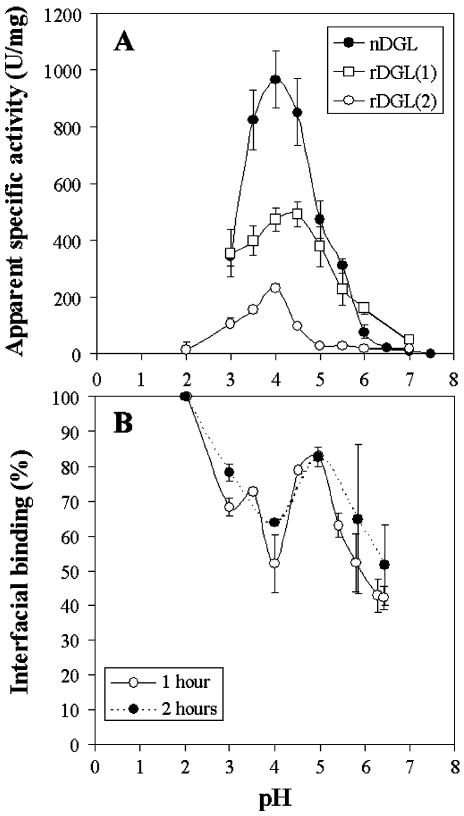

FIGURE 2: Effects of pH on the rDGL activity (A) and interfacial binding (B) using an Intralipid emulsion. (A) Activities were measured under optimized assay conditions (nDGL, rDGL(1); see the Experimental Procedures), as well as with Intralipid dispersed in a 150 mM NaCl and 2 mM NaTDC solution [rDGL(2)]. (B) rDGL partitioning between the water phase and the oil−water interface was measured after either 1 or 2 h of centrifugation at 10 000 rpm.

rDGL Adsorption at a Solid Hydrophobic Surface Determined by TIRF Spectroscopy. TIRF spectroscopy was used to monitor rDGL adsorption onto hydrophobic quartz slides prepared with dichoromethylsilane. Experiments were performed in the presence and absence of 2 mM bile salts (sodium taurodeoxycholate, NaTDC). In both cases, rDGL was found to bind to the hydrophobic solid surface, as shown by the increase in the surface fluorescence observed after applying a continuous flow of rDGL solution in the TIRF reaction chamber. In both cases, the surface fluorescence level was found to decrease when the TIRF reaction chamber was washed with buffer containing no rDGL, reflecting the occurrence of a reversible adsorption process. Data obtained without any bile salts were not suitable, however, for estimating the kinetic constants because of the discontinuous patterns of changing fluorescence intensity (data not shown). These variations in surface fluorescence intensity probably resulted from the adsorption of several layers of rDGL as well as from the unfolding process taking place at the hydrophobic interface. Similar findings were obtained when large rDGL concentrations in the micromolar range were

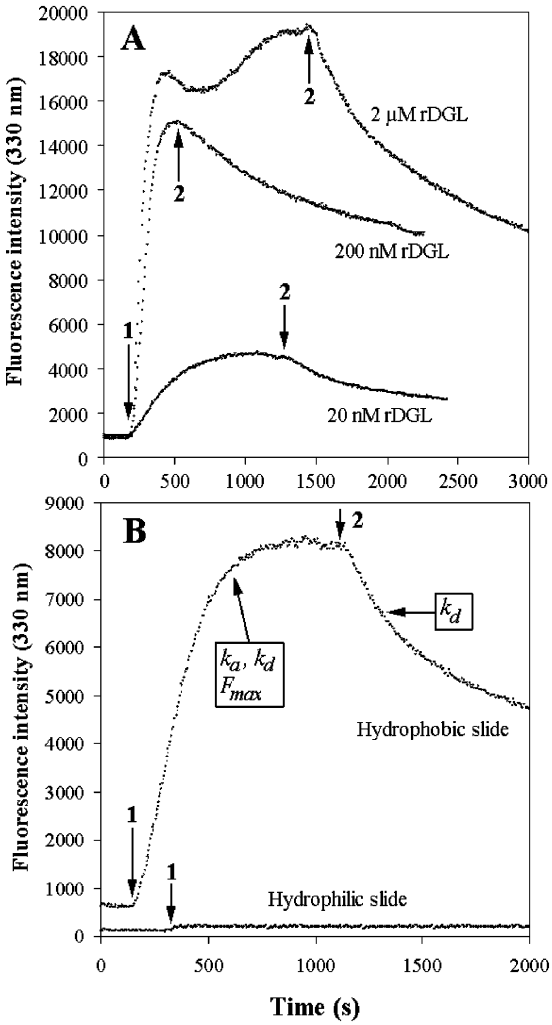

FIGURE 3: Setting up the experimental conditions for measuring the rDGL adsorption on a solid hydrophobic surface using TIRF. (A) rDGL adsorption (fluorescence intensity at 330 nm) on a hydrophobic quartz slide at various enzyme concentrations ranging from 20 nM to 2 μM. Experiments were performed in 150 mM NaCl, 2 mM NaTDC, and 10 mM citrate buffer at pH 6. Arrows 1 indicate the start of the rDGL flow in the TIRF reaction chamber. Arrows 2 indicate the start of the washing of the TIRF reaction chamber with the buffer without any rDGL. (B) rDGL adsorption (fluorescence intensity at 330 nm) on a hydrophobic quartz slide prepared with dichlorodimethylsilane versus an untreated hydrophilic quartz slide. Experiments were performed in 150 mM NaCl, 2 mM NaTDC, and 10 mM citrate buffer at pH 5, with a rDGL concentration of 20 nM. On the basis of the Langmuir adsorption model, the changes with time in the fluorescence intensity observed with the hydrophobic quartz slide and rDGL flow at a constant concentration were used to estimate the kinetic constants of the rDGL adsorption (k_a) and desorption (k_d) processes, as well as the maximum fluorescence intensity (F_{max}) that could be theoretically reached upon rDGL binding.

used (Figure 3A). The rDGL concentration had to be reduced to 20 nM to be able to record surface fluorescence variations compatible with a Langmuir adsorption model (Figure 3A). We checked that no increase in the surface fluorescence occurred when rDGL was injected into a TIRF reaction chamber containing a hydrophilic quartz slide, which showed that an increase in the surface fluorescence was associated with an adsorption of rDGL onto a hydrophobic surface (Figure 3B). Final experiments were all performed using a 20 nM rDGL solution prepared in either 10 mM citrate buffer (pH 4−7) or 10 mM phosphate buffer (pH 3) containing

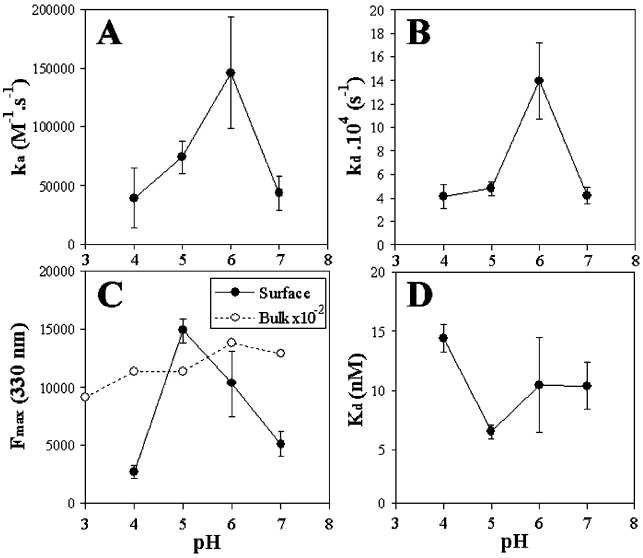

FIGURE 4: Effects of pH on the kinetic and dissociation constants of rDGL binding to a hydrophobic solid surface. The adsorption constant (k_a, A), the desorption constant (k_d, B), and the maximum surface fluorescence intensity at 330 nm resulting from rDGL adsorption (F_{max}, C) were estimated by curve-fitting experimental data points to the Langmuir adsorption equation. k_d was also determined independently from the desorption curve. The effects of pH on the fluorescence intensity of a 20 nM rDGL solution were also measured in bulk conditions (C). (D) Dissociation constant (K_d) of the rDGL binding process. TIRF experiments were performed in 150 mM NaCl, 2 mM NaTDC, and 10 mM citrate buffer at a rDGL concentration of 20 nM.

150 mM NaCl and 2 mM NaTDC. The effects of pH on the rDGL adsorption were studied in the pH range of 3−7, and the kinetic parameters were estimated by curve-fitting the surface fluorescence intensity increase with time (Figure 3B) to the Langmuir eq 1, after substituting the rDGL surface fluorescence for the surface concentration

$$F(t) = \frac{F_{max} k_a C}{k_a C + k_d}[1 - \exp(-(k_a C + k_d)t)] \qquad (1)$$

where k_a is the adsorption constant (in M^{-1} s^{-1}), k_d is the desorption constant (s^{-1}), $F(t)$ is the surface fluorescence intensity measured as a function of time, F_{max} is the maximum fluorescence intensity reached upon rDGL binding, and C is the constant rDGL concentration (20×10^{-9} M) in the bulk phase. The desorption constant (k_d) was also estimated by curve-fitting the surface fluorescence intensity variation with time when the TIRF reaction chamber was washed with a continuous flow of rDGL-free buffer (Figure 3B), using the following eq 2:

$$F(t) = F_0 \exp(-k_d t) \qquad (2)$$

where F_0 is the initial surface fluorescence. It was checked that k_d values obtained separately from eqs 1 and 2 were similar. The association k_a was also determined from the association phase using eq 1 and the k_d value, obtained separately from the dissociation phase and eq 2.

The kinetic constants (k_a and k_d) and the maximum surface fluorescence intensity (F_{max}) were all found to vary significantly with the pH level, and the maximum values were observed at acidic pH levels (parts A−C of Figure 4). The maximum adsorption (k_a = 147 860 M^{-1} s^{-1}) and desorption

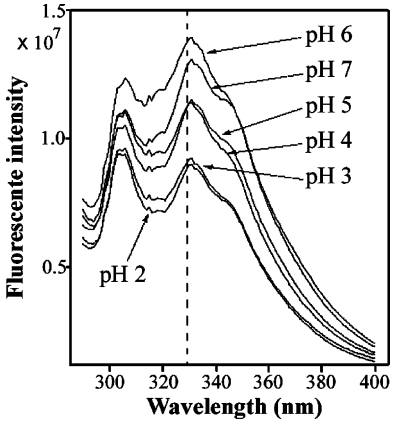

FIGURE 5: Effects of pH on the fluorescence spectrum of rDGL measured in bulk. Experiments were performed using 20 nM rDGL solutions prepared in either 150 mM NaCl, 2 mM NaTDC, and 10 mM citrate buffer (pH 4−7) or 150 mM NaCl, 2 mM NaTDC, and 10 mM phosphate buffer (pH 2 and 3).

($k_d = 139 \times 10^{-4}$ s^{-1}) constants were both obtained at pH 6, and the ratio between these values gave the lower dissociation constant at pH 5 ($K_d = k_d/k_a = 6.5$ nM; Figure 4D). In good agreement with this K_d value, the surface fluorescence intensity (F_{max}) showed a maximum value at pH 5 (Figure 4C).

To check that pH-dependent changes in the fluorescence actually reflected the adsorption of rDGL and not structural changes, the effects of pH on the rDGL fluorescence were also studied in bulk (Figure 5). The rDGL fluorescence spectrum showed an increase in the fluorescence intensity from pH 2 to 6, but the relative changes in the fluorescence intensity observed at 330 nm (1.5-fold increase) were lower than those observed with the surface fluorescence intensity measured with TIRF at the same emission wavelength (Figure 4C), with a 6-fold increase from pH 4 to 5.

QCM Measurements of the rDGL Adsorption onto a Hydrophobic Surface. The pH-dependent adsorption of rDGL onto a hydrophobic solid surface was also monitored using a QCM. Similar rDGL adsorption data were obtained both with and without bile salts (data not shown), but the rDGL adsorption process reached equillibrium considerably faster without bile salts than with 2 mM bile salts (10−20 min versus more than 60 min). These results probably reflect the fact that bile salts compete with gastric lipase for adsorption at the hydrophobic interface but do not impair the enzyme adsorption process, as previously established (*4*). The rDGL adsorption was found to be at a maximum at pH 5 (419 ± 25 ng cm^{-2}; Figure 6), and its pH dependency was similar to that previously observed in TIRF experiments (Figure 4C). To compare the TIRF and QCM results, the ratio between the maximum surface fluorescence intensity (TIRF) and the rDGL surface concentration (QCM) was calculated at pH 4−7. The values obtained (44, 35, 47, and 45, respectively) confirmed that both techniques gave similar results and that the surface fluorescence intensity measured with TIRF accurately reflects the rDGL adsorption at the hydrophobic solid surface.

Surface occupancy of the QCM hydrophobic surface (1.54 cm^2) was estimated from the rDGL surface concentration (ng cm^{-2}), rDGL molar mass (50 000 g mol^{-1}), and the section of a rDGL molecule deduced from its 3D structure (approximately 196×10^{-15} cm^2). At pH 5, where the maximum rDGL adsorption was observed, the hydrophobic surface was almost completely covered (99.1%) by a monolayer of rDGL (Table 1). Surface occupancy was only 26.5% at pH 7 and 14.7% at pH 4 (Table 1).

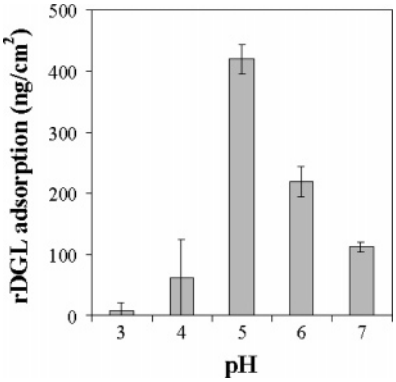

FIGURE 6: Effects of pH on the rDGL adsorption onto a hydrophobic solid surface measured using the QCM technique. Experiments were performed using 200 nM rDGL solutions prepared in either 150 mM NaCl, 2 mM NaTDC, and 10 mM citrate buffer (pH 4−7) or 150 mM NaCl, 2 mM NaTDC, and 10 mM phosphate buffer (pH 3).

Table 1: rDGL Adsorption onto a Hydrophobic Solid Surface Measured Using the QCM Technique and Surface Occupancy at Various pH Levels[a]

	rDGL adsorption		
pH	ng cm^{-2}	molecule cm^{-2}	surface occupancy (%)
3	9 ± 13	107×10^9	2.1
4	62 ± 63	746×10^9	14.7
5	419 ± 25	505×10^{10}	99.1
6	218 ± 25	263×10^{10}	51.6
7	112 ± 8	135×10^{10}	26.5

[a] The surface occupancy was estimated from the known area of the QCM flow cell, and the mean section of the rDGL molecule was deduced from its 3D structure (approximately 196×10^{-15} cm^2).

DISCUSSION

The experiments performed with the partly soluble VC4 substrate showed first that rDGL is active in solution, which means that the lid domain opens up in the water phase. This kinetic behavior has previously been found to occur in a large number of lipases possessing a lid controlling the access to the active site, and it probably reflects the ability of these lipases to be activated (opening of the lid) in solution in the presence of micellar aggregates of a partly soluble substrate (*13*). This kinetic property is supported by the fact that several 3D structures of lipases in the open conformation have been determined in the presence of detergent/micelles (*14*−*16*).

The maximum activity of rDGL on VC4 below its solubility limit was observed at neutral pH values (Figure 1A) and is therefore compatible with a catalytic mechanism involving a Ser-His-Asp catalytic triad. These data, along with the fact that the rDGL 3D structure did not show any specific structural features at the level of the catalytic triad (*6*), suggest that the catalytic triad of rDGL functions like that observed in chymotrypsin (*17*) and other serine hydrolases. Although the experiments performed with soluble VC4 suggest that the local pK_a of the catalytic histidine residue is close to 4.8 and that histidine pK_a values as low as 5.9 in

the lipolytic enzyme cutinase (*18*) and 5.3 in staphylococcal nuclease (*19*) were reported, the maximum activity of rDGL observed at pH 4.0 with long-chain triglycerides (Figure 2A) can hardly be explained by any specific structural feature of the active site and the environment of the catalytic triad.

When the VC4 concentration is above the solubility limit, the maximum activity of rDGL is shifted toward acidic pH values (Figure 1A), thus indicating that the presence of substrate aggregates affects the pH dependency of the rDGL activity. The large increase in the rDGL activity with the substrate concentration once the solubility limit (S) is exceeded also shows that rDGL is able to bind to and hydrolyze an insoluble substrate at a pH as low as 4.5 (Figure 1B). At pH 7.0, the rDGL activity shows no changes when the substrate concentration increases from 0.95 to 12 S, which indicates that rDGL probably remains in solution and is active only on the soluble fraction of VC4. These findings suggest that the adsorption of rDGL at a lipid−water interface might be higher at acidic pH values than at pH values near and above neutrality and that the optimum activity measured at pH 4.0 with long-chain triglycerides might only be "apparent". Contrary to soluble enzymes acting on a soluble substrate, lipases are soluble enzymes acting on an insoluble triglyceride substrate. The rate of substrate hydrolysis depends upon not only the formation of an interfacial enzyme−substrate complex (E*•S) and the catalytic constant (k_{cat}) but also the adsorption (k_a) and desorption (k_d) constants of the enzyme, as expressed in the kinetic model developed by Verger and De Haas (*7*, *20*). According to this model, the variations of apparent enzyme activity with pH might not only result from k_{cat} variations with pH but also from the variation of the enzyme−lipid interface dissociation constant K_d with pH. A maximum apparent activity at acidic pH levels can thus result from a minimum K_d value at low pH, although k_{cat} is at a maximum at high pH values.

This hypothesis was first tested by measuring the partitioning of rDGL between the water phase and the oil−water interface formed by an Intralipid emulsion (Figure 2B). These experiments were only "qualitative", because the partitioning was measured after at least 1 h of centrifugation and the lipolysis products might have affected the initial rDGL adsorption at the oil−water interface, for instance, at pH 4 where the highest activity is measured. These experiments nevertheless confirmed that the interfacial binding of rDGL was higher at low pH values (Figure 2B).

TIRF and QCM techniques were further used to study rDGL adsorption on a solid hydrophobic surface independently from the process of substrate hydrolysis. These experiments, like those with Intralipid, were performed in the presence of a micellar concentration of bile salts (2 mM NaTDC). Although gastric lipase mainly acts in the stomach where bile salts are not usually present, it also acts in the small intestine where it was found to be stable and active in the presence of a meal (*1*). Moreover, gastric lipase is not inhibited by bile salts, on the contrary to other lipases (*4*). In the standard *in vitro* assay of gastric lipase, bile salts are even required to prevent the interfacial denaturation of the enzyme at the oil−water interface (*21*). The optimum activity of gastric lipase at acidic pH was therefore observed in the presence of bile salts, and it seemed justified to assay gastric lipase adsorption under similar conditions. The TIRF data obtained showed that both rDGL adsorption and desorption constants are pH-dependent and that they are at a maximum at acidic pH levels. The lowest dissociation constant (6.5 nM) and the maximum surface fluorescence intensity were recorded at pH 5 (Figure 4). The QCM data obtained confirmed that a higher adsorption of rDGL occurred onto a hydrophobic surface at pH 5 (Figure 6), with a complete monolayer of rDGL covering this hydrophobic surface. The maximum adsorption of rDGL was not observed at its isolelectric point (6.6), contrary to what has often been said to occur in the literature on protein adsorption onto solid surfaces (*22*).

All of the above findings support the idea that the apparent maximum activity of rDGL at acidic pH levels is due to the efficient interfacial binding occurring at low pH values and the poor interfacial binding occurring at high pH values, where the enzyme should normally display its maximum turnover. It is possible that rDGL might show a much higher apparent activity if it were able to bind efficiently to a lipid−water interface at high pH values.

Purely hydrophobic solid surfaces can be a useful tool for investigating rDGL adsorption properties independently from substrate hydrolysis, but these surfaces do not mimick oil−water interfaces, at which several amphiphiles (such as phospholipids and lipolysis products) might be present. Experiments performed with Intralipid (soybean oil emulsified with egg lecithin) showed that rDGL interfacial binding is extremely high below pH 3 with all of the enzyme bound at the interface at pH 2 (Figure 2B), whereas TIRF and QCM experiments showed that the rDGL adsorption was lower below pH 5 (Figures 5 and 6). Although hydrophobic interactions seem to play an important role in the rDGL adsorption process, the fact that a higher adsorption of rDGL was observed at an oil−water interface at lower pH values (i.e., pH 2) might also mean that other types of interactions with the molecules present at the interface are involved. The effects of phospholipids and lipolysis products such as free fatty acids will have to be investigated in future studies with hydrophobic solid surfaces.

The pH-dependent adsorption of rDGL remains to be understood at the molecular level. As for other lipases, the rDGL 3D structure is characterized by the presence of a lid that controls the access to the active site. Under the open conformation of the lid, the 3D structure of rDGL shows a large hydrophobic surface surrounding the entrance of the active site (*6*). This finding is consistent with the strong rDGL affinity for hydrophobic interfaces observed. The surface potential of rDGL was calculated with the TITRA sofware program (*23*) at various pH values ranging from 2 to 7, and it was shown that (i) the large apolar ring surrounding the active-site cavity is preserved whatever the pH and (ii) that the protein is positively charged below pH 5. These findings do not explain, however, the fact that rDGL adsorption onto a solid hydrophobic surface is pH-dependent, shows an optimum at pH 5, and decreases below this pH value. Electrostatic interactions might also play a role. The bile salts present in the system are always negatively charged in the pH range investigated (2−7) because of their very low pK_a values (1.93−1.95; *24*). The bile-salt molecules present at the interface might interact with rDGL, which was found to contain several basic residues at the edge of its putative interfacial binding side. Such putative interactions

are unlikely to be affected at pH values below 5, where the rDGL is always positively charged. Moreover, because bile salts might also interact with rDGL in solution, it is difficult to determine how these putative interactions may induce rDGL desorption at pH levels below 5.

Intramolecular electrostatic interactions involving acidic residues might also contribute importantly to stabilizing the open conformation of the rDGL lid, which is required for rDGL adsorption to occur. Among the acidic residues found to be present in the lid, only Glu225 establishes a double interaction (<4 Å) with basic residues Lys4 and Arg229 in the open conformation of rDGL. These interactions do not occur in the closed conformation of HGL (see PDB 1HGL; *5*). At pH values below the glutamate pK_a (4.3), it is possible that the electrostatic interactions between Glu225 and basic residues may be reduced. Key residues involved in electrostatic interactions stabilizating the open conformation of the lid have previously been observed in human pancreatic lipase (*25*) and *Thermomyces lanuginosus* lipase (*26*). Mutagenesis experiments remain to be performed with rDGL to check the role of Glu225.

In conclusion, the present data show that gastric lipase is able to hydrolyze the ester bonds of a soluble substrate (VC4) in line with the classical mechanism described in the case of serine hydrolases in solution; they therefore support and extend the results of structural studies, in which the catalytic triad of gastric lipase was not found to differ significantly from those observed in other lipases/esterases. Experiments performed with the soluble VC4 substrate suggest however that the pK_a of the active-site histidine might be unusually low (around 4.8), but this is not sufficient to explain the maximum activity of rDGL observed at pH 4 with long-chain triglycerides. This "apparent" maximum activity observed at acidic pH when rDGL is acting on an insoluble substrate is probably due to the fact that the enzyme adsorption process at the lipid−water interface is pH-dependent and constitutes the limiting step in the overall interfacial catalytic process carried out by gastric lipase. Because mainly hydrophobic interactions contribute to rDGL adsorption at a hydrophobic interface, the pH dependency of the adsorption process might result from electrostatic interactions stabilizing the open conformation of the lid and, thus, the exposure of a large hydrophobic surface surrounding the active site on one side of the gastric lipase molecule. This hypothesis applies to the interactions between rDGL and a hydrophobic solid surface. With triglyceride emulsions coated with phospholipids, such as Intralipid, the interfacial binding of rDGL increases inversely with the pH (Figure 2B), probably because additional electrostatic interactions between rDGL and phospholipids are involved in stabilizing rDGL in the open conformation at the oil−water interface. Further studies are still required, however, to unravel the effects of the pH on the interfacial adsorption of gastric lipase at the molecular level.

Another hypothesis for explaining the acidic activity of some triglyceride lipases was proposed very recently (*27*). Because the pK_a value of the catalytic histidine of cutinase measured in the absence of the substrate was not consistent with the detected acid activity, Poulsen et al. proposed a novel model for the electrostatics in the active site of cutinase that could explain the observed acidic activity: the classical definition of pH in bulk solution is not applicable to the active-site environment of a lipase when the active site is inaccessible to the solvent and chemical communication because of the adsorption of the lipase at a lipid interface. In small restricted volumes, the pH might be quantized and different from the overall pH value of the enzyme bulk environment.

ACKNOWLEDGMENT

We are grateful to Dr. Pierre Dorfman and Dr. Dominique Mison (Meristem Therapeutics, Clermont-Ferrand, France) for providing the rDGL produced in transgenic plants. The authors thank Francine Ferrato for carrying out the purification of rDGL, Jessica Blanc for revising the English manuscript, and Dr. Sonia Longhi for critical reading of the manuscript.

REFERENCES

1. Carrière, F., Barrowman, J. A., Verger, R., and Laugier, R. (1993) Secretion and contribution to lipolysis of gastric and pancreatic lipases during a test meal in humans, *Gastroenterology 105*, 876−888.
2. Ville, E., Carriere, F., Renou, C., and Laugier, R. (2002) Physiological study of pH stability and sensitivity to pepsin of human gastric lipase, *Digestion 65*, 73−81.
3. Carrière, F., Moreau, H., Raphel, V., Laugier, R., Bénicourt, C., Junien, J.-L., and Verger, R. (1991) Purification and biochemical characterization of dog gastric lipase, *Eur. J. Biochem. 202*, 75−83.
4. Lengsfeld, H., Beaumier-Gallon, G., Chahinian, H., De Caro, A., Verger, R., Laugier, R., and Carrière, F. (2004) Physiology of gastrointestinal lipolysis and therapeutical use of lipases and digestive lipase inhibitors, in *Lipases and Phospholipases in Drug Development* (Müller, G., and Petry, S., Eds.) pp 195−229, Wiley-VCH, Weinheim, Germany.
5. Roussel, A., Canaan, S., Egloff, M. P., Riviere, M., Dupuis, L., Verger, R., and Cambillau, C. (1999) Crystal structure of human gastric lipase and model of lysosomal acid lipase, two lipolytic enzymes of medical interest, *J. Biol. Chem. 274*, 16995−17002.
6. Roussel, A., Miled, N., Berti-Dupuis, L., Riviere, M., Spinelli, S., Berna, P., Gruber, V., Verger, R., and Cambillau, C. (2002) Crystal structure of the open form of dog gastric lipase in complex with a phosphonate inhibitor, *J. Biol. Chem. 277*, 2266−2274.
7. Verger, R., Mieras, M. C. E., and de Haas, G. H. (1973) Action of phospholipase A at interfaces, *J. Biol. Chem. 248*, 4023−4034.
8. Baron, M. H., Revault, M., Servageant-Noinville, S., Abadie, J., and Quiquampoix, H. (1999) Chymotrypsin adsorption on Montmorillonite: enzymatic activity and kinetic FTIR structural analysis, *J. Colloid Interface Sci. 214*, 319−332.
9. Snabe, T., Neves-Petersen, M. T., and Petersen, S. B. (2005) Enzymatic lipid removal from surfaces−Lipid desorption by a pH-induced "electrostatic explosion", *Chem. Phys. Lipids 133*, 37−49.
10. Buijs, J., and Hlady, V. (1997) Adsorption kinetics, conformation, and mobility of the growth hormone and lysozyme on solid surfaces, studied with TIRF, *J. Colloid Interface Sci. 190*, 171−181.
11. Sauerbrey, G. A. (1959) Verwendung von Schwingquarzen zur Wägung dünner Schichten und zur mikrowägung, *Z. Phys. 155*, 206−222.
12. Höök, F., Rodahl, M., Kasemo, B., and Brzezinski, P. (1998) Structural changes in hemoglobin during adsorption to solid surfaces: Effect of pH, ionic strength, and ligand binding, *Proc. Natl. Acd. Sci. U.S.A. 95*, 12271−12276.
13. Nini, L., Sarda, L., Comeau, L. C., Boitard, E., Dubes, J. P., and Chahinian, H. (2001) Lipase-catalysed hydrolysis of short-chain substrates in solution and in emulsion: A kinetic study, *Biochim. Biophys. Acta 1534*, 34−44.
14. van Tilbeurgh, H., Egloff, M.-P., Martinez, C., Rugani, N., Verger, R., and Cambillau, C. (1993) Interfacial activation of the lipase−procolipase complex by mixed micelles revealed by X-ray crystallography, *Nature 362*, 814−820.
15. Hermoso, J., Pignol, D., Kerfelec, B., Crenon, I., Chapus, C., and Fontecilla-Camps, J. C. (1996) Lipase activation by nonionic

detergents. The crystal structure of the porcine lipase−colipase−tetraethylene glycol monooctyl ether complex, *J. Biol. Chem. 271*, 18007−18016.
16. Hermoso, J., Pignol, D., Penel, S., Roth, M., Chapus, C., and Fontecilla-Camps, J. C. (1997) Neutron crystallographic evidence of lipase−colipase complex activation by a micelle, *EMBO J. 16*, 5531−5536.
17. Blow, D. M. (1971) The structure of chymotrypsin, in *The Enzymes* (Boyer, P. D., Ed.) pp 185−212, Academic Press, New York.
18. Prompers, J. J., Groenewegen, A., Hilbers, C. W., and Pepermans, H. A. (1999) Backbone dynamics of Fusarium solani pisi cutinase probed by nuclear magnetic resonance: The lack of interfacial activation revisited, *Biochemistry 38*, 5315−5327.
19. Mehler, E. L., Fuxreiter, M., Simon, I., and Garcia-Moreno, E. B. (2002) The role of hydrophobic microenvironments in modulating pK_a shifts in proteins, *Proteins: Struct., Funct., Genet. 48*, 283−292.
20. Verger, R., and de Haas, G. H. (1973) Enzyme reactions in a membrane model. 1: A new technique to study enzyme reactions in monolayers, *Chem. Phys. Lipids 10*, 127−136.
21. Gargouri, Y., Piéroni, G., Rivière, C., Saunière, J.-F., Lowe, P. A., Sarda, L., and Verger, R. (1986) Kinetic assay of human gastric lipase on short- and long-chain triacylglycerol emulsions, *Gastroenterology 91*, 919−925.
22. Norde, W. (1986) Adsorption of proteins from solution at the solid−liquid interface, *Adv. Colloid Interface Sci. 25*, 267−340.
23. Petersen, S. B., Fojan, P., Petersen, E. I., and Petersen, M. T. (2001) The thermal stability of the Fusarium solani pisi cutinase as a function of pH, *J. Biomed. Biotechnol. 1*, 62−69.
24. Small, D. M. (1971) The physical chemistry of cholanic acid, in *The Bile Acids* (Nain, P. P., and Kritchevsky, D., Eds.) pp 249−356, Plenum Press, New York.
25. Bezzine, S., Ferrato, F., Ivanova, M. G., Lopez, V., Verger, R., and Carriere, F. (1999) Human pancreatic lipase: Colipase dependence and interfacial binding of lid domain mutants, *Biochemistry 38*, 5499−5510.
26. Brzozowski, A. M., Savage, H., Verma, C. S., Turkenburg, J. P., Lawson, D. M., Svendsen, A., and Patkar, S. (2000) Structural origins of the interfacial activation in *Thermomyces* (*Humicola*) *lanuginosa* lipase, *Biochemistry 39*, 15071−15082.
27. Poulsen, K. R., Snabe, T., Petersen, E. I., Fojan, P., Neves-Petersen, M. T., Wimmer, R., and Petersen, S. B. (2005) Quantization of pH: Evidence for acidic activity of triglyceride lipases, *Biochemistry 44*, 11574−11580.

BI0518803